NASA Technical Memorandum 105549

Comparison of GLIMPS and HFAST Stirling Engine Code Predictions With Experimental Data

Steven M. Geng and Roy C. Tew
Lewis Research Center
Cleveland, Ohio

Prepared for the
27th Intersociety Energy Conversion Engineering Conference
cosponsored by the SAE, ACS, AIAA, ASME, IEEE, AIChE, and ANS
San Diego, California, August 3–7, 1992

NASA

Table 1. RE-1000 and SPRE Design Operating Conditions

Parameter		RE-1000 Rdg #1010	SPRE Rdg #1215
Working Fluid		Helium	Helium
Pressure	MPa	7.0	15.0
Ave. Heater Temp	°C	600	341
Ave. Cooler Temp	°C	57	33
Frequency	Hz	30.1	102.3
Displacer Phase	°	57.5	76.4
Piston Stroke	cm	2.60	2.02
Displacer Stroke	cm	2.34	2.13

GLIMPS AND HFAST STIRLING SIMULATIONS

GLIMPS is a constrained mode simulation that uses a globally implicit technique to solve a system of algebraic equations simultaneously. The algebraic equations are finite difference representations of the governing differential equations. GLIMPS is a one-dimensional model comprised of up to 7 components relating to the working space of a Stirling cycle machine. Each component is divided into a number of computational-cells. The computational domain is broken into discrete time nodes as well. The user specifies the number of computational-cells and time nodes used in the model. GLIMPS, developed by Gedeon Associates, recently has been upgraded to version 4.0[4,5].

HFAST is a constrained mode simulation that assumes the variables are harmonic functions of time. The solution is found by solving a system of nonlinear, algebraic equations which are created by substituting harmonic functions in the governing differential equations. HFAST is a one-dimensional model comprised of a variable number of components relating to the working space of a Stirling cycle machine. Each component is divided into a number of control-volumes. The user specifies the number of components and control-volumes used in the model. HFAST, written by Mechanical Technology, Inc., has recently been upgraded to version 2.0[6].

GLIMPS AND HFAST ENGINE MODELS

GLIMPS RE-1000 MODEL - Two computational-cells were used each in the cooler, regenerator manifolds, and heater. Four computational-cells were used in the regenerator. Twelve time nodes per cycle were used for all predictions. GLIMPS does not allow all connecting-ducts to be modeled directly. The expansion-space-to-heater connecting-duct volume was lumped with the expansion-space. The compression-space-to-cooler connecting-duct volume was lumped with the compression-space.

Portions of the RE-1000 regenerator manifolds are not in the working-space gas flow stream. These portions were lumped with the expansion and compression-space volumes.

The heater and cooler temperatures were assumed constant over their length. This assumption was made since no experimental data were taken to clearly define the wall temperature gradient. The actual RE-1000 heater and cooler temperatures were not uniform.

HFAST RE-1000 MODEL - Two control-volumes were used each in the cooler, regenerator manifolds, and heater. Four control-volumes were used in the regenerator. One control-volume was used for the expansion-space-to-heater connecting-duct while two control-volumes were used for the compression-space-to-cooler connecting-duct; note that, unlike GLIMPS, these connecting-ducts were not lumped with the expansion and compression-spaces.

To be consistent with GLIMPS, the portions of the regenerator manifold volumes not in the working-space gas flow stream were lumped with the expansion and compression-space volumes.

The temperatures of the heater and cooler were assumed constant over their length. This assumption was made for the reason explained for the GLIMPS model.

GLIMPS SPRE MODEL - Four computational-cells were used each in the cooler, regenerator, and heater. Two computational-cells were used in each regenerator manifold. No connecting-duct exists between the expansion-space and heater. The compression-space-to-cooler connecting-duct volume and surface area were lumped in with the compression-space.

HFAST SPRE MODEL - Four control-volumes were used each in the cooler, regenerator, and heater. Only one control-volume could be used for each regenerator manifold. Two could not be used since HFAST limits the total number of control-volumes in the model. The one control-volume manifold models should not cause difficulties when comparing the HFAST and GLIMPS predictions since the SPRE manifolds are small. Two control-volumes were used for the compression-space-to-cooler connecting-duct which is extremely large; note that, unlike GLIMPS, this connecting-duct volume was not lumped with the compression-space.

CODE CALIBRATION

Calibration parameters are defined as the set of multiplication factors and coefficients required to adjust predicted pressure drops, heat transfer, and gas flow rates. The term factor refers to the subset of dimensionless calibration parameters while the term coefficient refers to the subset of calibration parameters that have physical properties. The parameters used to calibrate GLIMPS and HFAST are shown in Table 2. Note that no leakage coefficients were used to calibrate GLIMPS. A leakage model has been added to the main simulation of GLIMPS 4.0. However, it was not operational in the beta version of the code that was used for this paper. Leakage calculations were made in the GLIMPS postprocessor. These leakages could not be used to calibrate GLIMPS since they have no affect on the engine pressure waves calculated in the main simulation.

A performance map was generated for each code by varying each calibration parameter individually. The maps were used as a guide to adjust the parameters to bring the code predictions into better agreement with the test data.

The performance parameters of interest for the RE-1000 calibration included: 1) engine power, 2) gross engine thermal efficiency, 3) compression-space pressure amplitude, 4) compression-space pressure phase angle, 5) power input to engine heater, and 6) power rejected to the coolant.

Table 2. GLIMPS and HFAST Calibration Parameters

Calibration Parameters		GLIMPS Nominal	GLIMPS Final RE-1000	GLIMPS Final SPRE	HFAST Nominal	HFAST Final RE-1000	HFAST Final SPRE
CS H_Mult		1.0	**1.6**	**0.2**	1.0	**3.0**	1.0
ES H_Mult		1.0	**1.6**	**0.2**	1.0	**3.0**	1.0
C H_Mult		A1	**0.7**	1.0	A1	**0.7**	1.0
R H_Mult		1.0	1.0	1.0	1.0	**1.5**	**.85**
H H_Mult		1.0	1.0	1.0	1.0	1.0	1.0
C F_Mult		1.0	1.0	1.0	1.0	1.0	1.0
R F_Mult		1.0	**1.4**	1.0	1.0	1.0	1.0
H F_Mult		1.0	**2.0**	1.0	1.0	1.0	1.0
ES-CS L_Coef	m3	-	-	-	A2	**4.0E-14**	3.4E-13
CS-Pm L_Coef	m3	-	-	-	A3	**2.9E-14**	1.3E-13
CS CP L_Coef	m2	-	-	-	A4	-6.6E-8	-1.7E-6

Key:

A1	= 8.7 E-01 for RE-1000;	1.0 E+00 for SPRE	
A2	= 0.0 E+00 for RE-1000;	3.4 E-13 for SPRE	
A3	= 9.0 E-16 for RE-1000;	1.3 E-13 for SPRE	
A4	= -6.6 E-08 for RE-1000;	-1.7 E-06 for SPRE	
C	= Cooler	CP	= Center Port
CS	= Compression Space	ES	= Expansion Space
F_Mult	= Friction Mult. Fact.	H	= Heater
H_Mult	= Heat Trans. Mult. Fact.	L_Coef	= Leakage Coef.
Pm	= Mean Pressure	R	= Regenerator

The performance parameters of interest for the SPRE calibration included: 1) piston PV (Pressure-Volume) power, 2) piston PV efficiency, 3) compression-space pressure amplitude, 4) compression-space pressure phase angle, 5) power input to engine heater, and 6) power rejected to the coolant.

For the RE-1000, the engine power and gross engine thermal efficiency were the most accurate of the experimental power and efficiency measurements. For the SPRE, engine power and thus gross engine thermal efficiency measurements were not possible due to the instrumentation. The linear alternator is an integral part of the SPRE power piston. The engine power is defined by ASME[3] as the power delivered to the output convertor by the engine (i.e. engine power = indicated power - piston and displacer losses). The linear alternator is the output convertor for the SPRE. The only power and efficiency measurements that could be compared with the code predictions on an equivalent basis were piston PV power and efficiency.

GLIMPS and HFAST were calibrated at the design operating conditions of each engine (RE-1000 Rdg #1010 and SPRE Rdg #1215). The calibration parameters were adjusted until all or most of the performance parameters of interest were within the error bands of the test data. No attempt was made to further calibrate within the error bands or over a range of operating conditions. The nominal and final calibration parameters are shown in Table 2.

COMPARISON OF ENGINE THERMODYNAMICS

GLIMPS and HFAST predictions are compared in Tables 3 and 4. The experimental data are shown for each engine at its design operating conditions. Uncalibrated and calibrated predictions are shown for each code.

RE-1000 COMPARISONS - Table 3 shows the code predictions for the RE-1000 at its design operating conditions. The engine power and gross engine thermal efficiency were two of the six performance parameters for which the codes were calibrated. Note that HFAST does not directly calculate engine power. To be consistent with GLIMPS, the piston gas spring hysteresis loss (not shown separately in the Tables) was subtracted from the piston PV power to obtain the HFAST engine power.

Table 3. RE-1000 Performance at Design Operating Conditions

Parameter		Test Data #1010	UNCALIBRATED GLIMPS	UNCALIBRATED HFAST	CALIBRATED GLIMPS	CALIBRATED HFAST
Indicated Power	W		1201	1317	976	1212
Indicated Engine Efficiency	%		31.3	31.1	26.9	32.4
Engine Power	W	866	1031	1225	885	891
Gross Engine Thermal Eff	%	23.8	26.9	28.9	24.4	23.8
Net Displacer PV	W		111	34	34	42
CS Pressure Amplitude	MPa	1.15	1.16	1.14	1.13	1.14
CS Pressure Phase Angle	°	-15.7	-16.7	-19.9	-14.8	-14.3
Parasitic Heat Loss	W		308	301	301	234
Parasitic Power Loss	W		60	58	57	279
Heat Input	W	3643	3836	4238	3623	3737
Heat Rejected	W	2736	2694	2947	2704	2773
Carnot Efficiency	%	62.2	62.2	62.2	62.2	62.2
Available Power	W	2266	2386	2636	2253	2324
Lost Available Power (LAP)	W		1185	1319	1277	1112
Itemized LAP:						
Viscous Dissipation	W		69	105	98	93
Gas-to-Wall Heat Transfer:						
In Phase With aT	W		627	599	690	504
Leading aT	W		-	70	-	74
Gas Conduction	W		99	10	96	10
Mixing Loss	W		-	127	-	102
Parasitic Heat Loss	W		192	187	187	145
Total	W		987	1098	1071	928
% Error	%		-16.7	-16.8	-16.1	-16.5

Ideally, the net displacer PV power should be zero for all predictions. A non-zero value indicates a mismatch between the predicted thermodynamics and the assumed dynamics (i.e. a positive net displacer PV indicates that more power is going into the displacer than is consumed by displacer losses).

The parasitic heat loss prediction includes the following: 1) wall conduction, 2) displacer shell conduction, 3) displacer internal gas conduction, 4) displacer shuttle loss, and 5) displacer appendix gap loss. The parasitic power loss prediction includes the following: 1) piston center-port leakage, 2) piston seal leakage, 3) piston gas-spring hysteresis, 4) displacer center-port leakage, 5) displacer gas-spring seal leakage, and 6) displacer gas-spring hysteresis. The heat input and heat rejected predictions include the effects of the parasitic heat losses.

Available power was calculated by multiplying the heat input by the Carnot efficiency. Lost available power (LAP) was then calculated by subtracting the indicated power from the available power. HFAST predicted higher available power for both uncalibrated and calibrated comparisons. HFAST predicted higher LAP for the uncalibrated comparison but lower LAP for the calibrated comparison.

Thermodynamic 2nd law LAP analysis was recently incorporated in GLIMPS and HFAST to permit separation of irreversibilities due to different loss mechanisms. The resulting irreversibilities or available power losses, itemized in Table 3, are: 1) viscous dissipation loss, 2) gas-to-wall heat transfer in phase with the temperature difference between the mean gas and wall temperatures, 3) gas-to-wall heat transfer leading the temperature difference, 4) gas axial conduction, 5) gas mixing loss, and 6) parasitic heat loss.

In general, heat transfer is out of phase with the mean-gas-to-wall temperature difference in Stirling cycle machines.

The gas-to-wall heat transfer in phase with temperature difference shown in Table 3 (and 4) was calculated based on steady-flow heat transfer correlations which do not account for this phase shift. HFAST calculates an additional heat transfer which leads temperature difference based on a correlation developed by Lee[7]. This additional heat transfer is intended to correct the steady-flow heat transfer for phase shift. In contrast, GLIMPS does not attempt to correct the steady-flow heat transfer for phase shift.

GLIMPS does not calculate gas mixing losses at the component interfaces. GLIMPS assumes a continuous temperature distribution between computational-cells (unlike HFAST). According to Gedeon, GLIMPS accounts for the mixing losses under enhanced gas axial conduction.

Available power loss due to parasitic heat loss was computed by multiplying total parasitic heat loss by the Carnot efficiency. In an ideal engine, the parasitic heat loss would contribute to indicated power. Indicated power would be larger by the parasitic heat loss multiplied by the Carnot efficiency.

In the uncalibrated comparisons between GLIMPS and HFAST, GLIMPS predicted lower viscous dissipation and gas-to-wall heat transfer, but higher gas conduction loss. The parasitic heat losses were about the same.

In the calibrated comparisons, GLIMPS predicted higher gas-to-wall heat transfer, gas conduction, and parasitic heat losses. Although not shown in the tables, higher GLIMPS gas-to-wall heat transfer losses are largely due to the larger cylinder heat transfer predicted by GLIMPS. The viscous dissipation loss was roughly the same for the two codes.

The itemized available power losses were summed and checked against the previous LAP calculation. The percent error in the summation of these itemized losses ranged from -16.1% to -16.8%. Thus, it appears that some itemized losses are being underestimated or completely overlooked.

SPRE COMPARISONS - Table 4 shows the code predictions for the SPRE at its design operating conditions. Note that the accuracy of the experimental heater and cooler-tube temperatures is questionable for the SPRE. The predicted performance of the SPRE is extremely sensitive to temperature ratio. Any error in heater or cooler temperature has a large effect on calculated performance.

The piston PV power and efficiency were two of the performance parameters for which the codes were calibrated. GLIMPS predicted a significantly lower piston PV power and efficiency than HFAST in the uncalibrated comparison. The GLIMPS piston PV power and efficiency were only slightly higher in the calibrated comparison.

The total parasitic heat and power losses for the SPRE include the same losses as for the RE-1000. The SPRE has an additional displacer gas spring and several more leakage paths than the RE-1000. These additional losses have been taken into account. HFAST predicts significantly larger parasitic heat and power losses for both the uncalibrated and calibrated comparisons.

LAP for the SPRE predictions were re-calculated by summing the individual losses. The available power losses for the SPRE are itemized in Table 4. The percent error in the LAP calculations ranged from -0.6% to -17.3%.

Table 4. SPRE Performance at Design Operating Conditions

Parameter		Test Data #1215	UNCALIBRATED		CALIBRATED	
			GLIMPS	HFAST	GLIMPS	HFAST
Indicated Power	W		12310	17359	15740	17012
Indicated Engine Efficiency	%		19.8	28.7	24.9	27.1
Piston PV Power	W	12800	9702	12839	13021	12532
Piston PV Efficiency	%	20.3	15.6	21.2	20.6	20.0
Engine Power	W		9015	12152	12334	11845
Net Displacer PV	W		-84	411	-56	414
CS Pressure Amplitude	MPa	1.73	1.62	1.65	1.64	1.63
CS Pressure Phase Angle	°	-8.0	-7.4	-8.4	-9.6	-8.3
Parasitic Heat Loss	W		941	2861	954	2953
Parasitic Power Loss	W		3381	4144	3468	4085
Heat Input	W	63120	62167	60584	63130	62798
Heat Rejected	W	52330	53239	46177	50847	48681
Carnot Efficiency	%	50.1	50.1	50.1	50.1	50.1
Available Power	W	31623	31146	30353	31628	31462
Lost Available Power (LAP)	W		18836	12994	15838	14450
Itemized LAP:						
Viscous Dissipation	W		2210	3115	2196	3103
Gas-to-Wall Heat Transfer:						
In Phase With ΔT	W		11652	6064	8769	6655
Leading ΔT	W		-	712	-	704
Gas Conduction	W		1698	52	1704	53
Mixing Loss	W		-	1534	-	1687
Parasitic Heat Loss	W		471	1433	478	1479
Total	W		16031	12910	13147	13681
% Error	%		-14.9	-0.6	-17.3	-5.3

In both uncalibrated and calibrated comparisons, GLIMPS predicted lower viscous dissipation and parasitic heat losses but much higher gas-to-wall heat transfer and gas conduction losses. Again, the high GLIMPS gas-to-wall heat transfer losses are due to much higher cylinder heat transfer.

COMPARISON OF POWER AND EFFICIENCY

Comparisons of predicted and measured data are shown as a function of piston amplitude in Figs. 3 through 10. Error bars have been placed on the experimental data. The error bars indicate the measurement error associated with each reading.

Figure 3 shows the uncalibrated engine power predictions for the RE-1000. Both codes over-predicted the power over the range of piston amplitudes modeled. GLIMPS and HFAST predicted a drop-off in the rate of increase in power at the higher amplitudes. The test data showed a linear increase in engine power with piston amplitude. The reason for this drop-off is not clear.

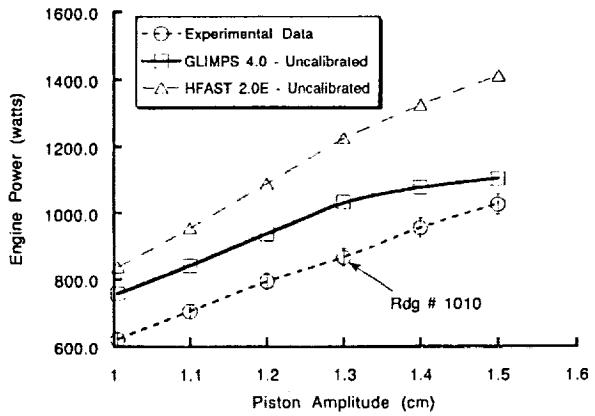

Figure 3 - RE-1000 Engine Power vs Piston Amplitude (Uncalibrated Predictions)

Figure 4 shows the uncalibrated gross engine thermal efficiency predictions for the RE-1000. Both codes over-predicted the efficiency over the entire range of piston amplitudes modeled. GLIMPS predicted a decrease in efficiency with increasing piston amplitude while HFAST predicted an efficiency curve with a trend similar to the test data. This difference in behavior indicates that at least one loss predicted by GLIMPS is overly sensitive to piston stroke.

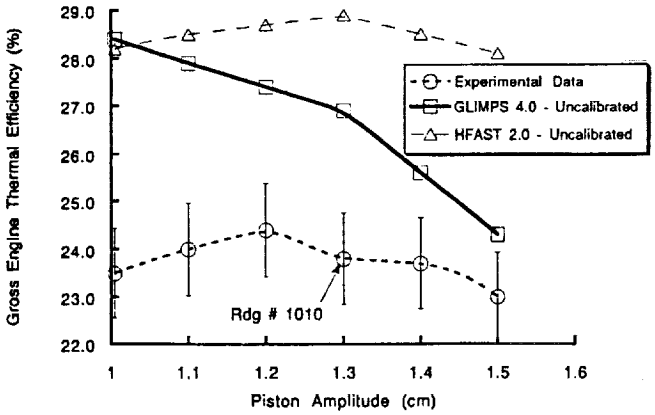

Figure 4 - RE-1000 Gross Engine Thermal Efficiency vs Piston Amplitude (Uncalibrated Predictions)

Figure 5 shows the calibrated engine power predictions for the RE-1000. Agreement with the data was much improved at design and lower piston amplitudes; at higher amplitudes, the drop-off in the rate of predicted power increase is still apparent.

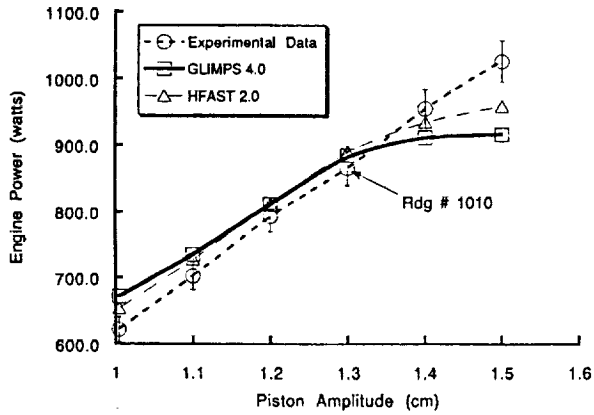

Figure 5 - RE-1000 Engine Power vs Piston Amplitude (Calibrated Predictions)

Figure 6 shows the calibrated gross engine thermal efficiency predictions for the RE-1000. Both codes over-predicted efficiency at low amplitudes and under-predicted efficiency at high amplitudes. Note that in the uncalibrated predictions shown in Fig. 4, the trend of the HFAST efficiency curve matched the trend of the data. Each calibration parameter was varied to determine which one shifted the trend. All parameters caused the efficiency curve to shift. These results indicate that the codes are incorrectly predicting a loss or losses for which no calibration parameter currently exists.

Figure 7 shows the uncalibrated piston PV power predictions for the SPRE. GLIMPS significantly under-predicted power over the range of piston amplitudes modeled. The HFAST predictions were within the experimental error bars over the entire range. Note that evolutionary changes to HFAST have been guided by SPRE data, and an earlier version of HFAST was used to design this engine.

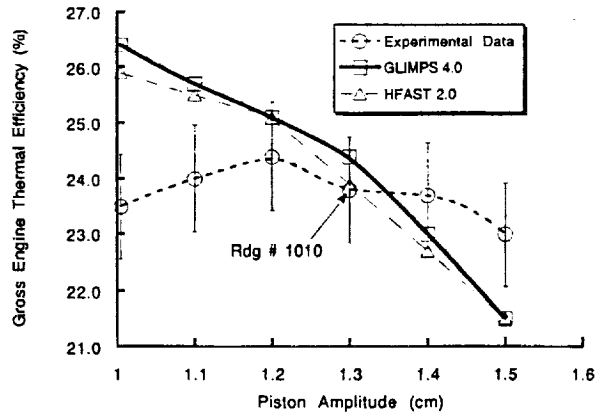

Figure 6 - RE-1000 Gross Engine Thermal Efficiency vs Piston Amplitude (Calibrated Predictions)

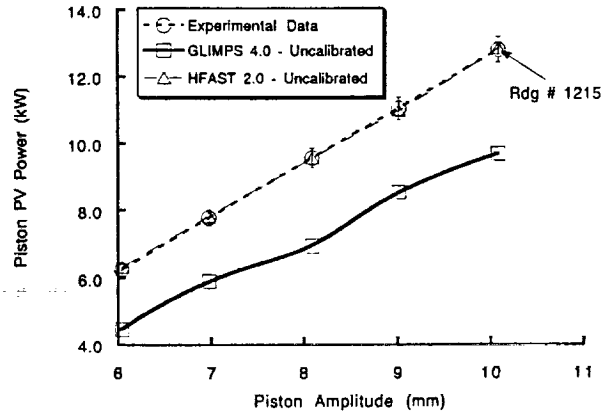

Figure 7 - SPRE Piston PV Power vs Piston Amplitude (Uncalibrated Predictions)

Figure 8 shows the uncalibrated piston PV efficiency predictions for the SPRE. GLIMPS significantly under-predicted efficiency while HFAST slightly over-predicted efficiency. The waviness in the GLIMPS efficiency curve may be due to numerical error.

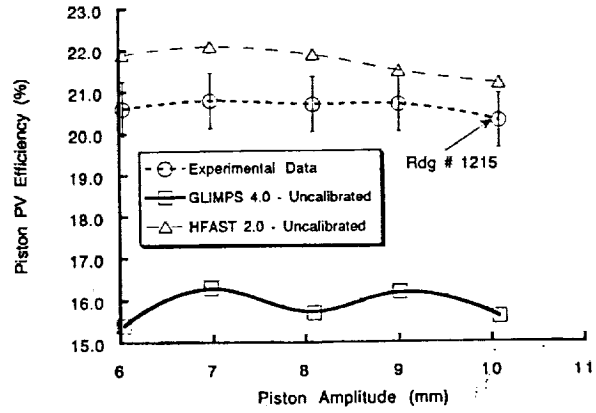

Figure 8 - SPRE Piston PV Efficiency vs Piston Amplitude (Uncalibrated Predictions)

Figure 9 shows the calibrated piston PV power predictions for the SPRE. GLIMPS under-predicted power at the low piston amplitudes. The agreement between the GLIMPS predictions and the experimental data was good at the higher piston amplitudes. The HFAST predictions were within the experimental error bars over the range of piston amplitudes modeled.

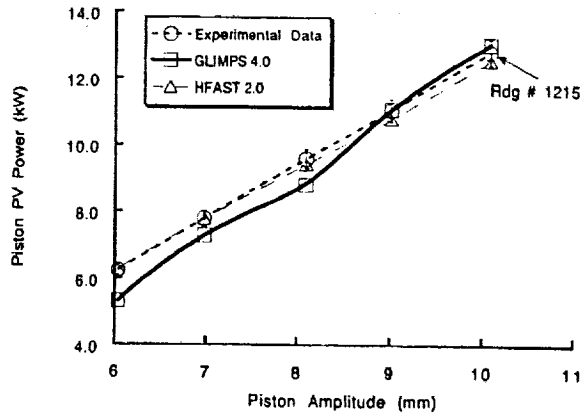

Figure 9 - SPRE Piston PV Power vs Piston Amplitude (Calibrated Predictions)

Figure 10 shows the calibrated piston PV efficiency predictions for the SPRE. GLIMPS significantly under-predicted efficiency at the low piston amplitudes. The HFAST predictions were within the experimental error bars over most of the range of piston amplitudes modeled. Although the calibration brought both codes into agreement with the data at the design piston amplitude (10 mm), the trends of the predicted efficiency curves seemed worse.

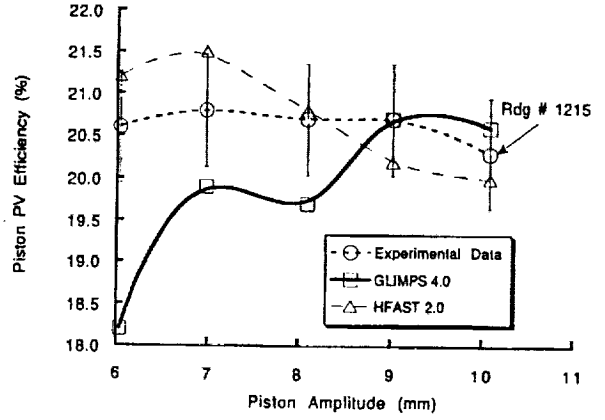

Figure 10 - SPRE Piston PV Efficiency vs Piston Amplitude (Calibrated Predictions)

CONCLUDING REMARKS

GLIMPS and HFAST loss comparisons disagree in magnitudes of losses. GLIMPS predicts higher gas-to-wall heat transfer in phase with temperature difference primarily due to larger cylinder heat transfer. GLIMPS also predicts higher gas conduction due to its enhanced conductivity model. The differences in predicted mixing losses can be attributed to the difference in assumptions about spatial variations of temperature. These differences in losses can cause the codes to optimize engine designs differently.

Both codes require engine-specific calibration parameters to bring predictions and experimental data into agreement. It would be desirable to obtain one set of calibration parameters for each code that would allow various Stirling engines to be modeled accurately. However, calibration experience suggests that a "best fit" set of calibration parameters is currently not obtainable.

The results documented in this paper indicate several areas where the codes could be improved. The cylinder heat transfer correlations for both codes should be re-evaluated. Work is currently underway to experimentally measure cylinder heat transfer in Stirling machine cylinders. Empirical correlations should be incorporated in both GLIMPS and HFAST when they become available.

GLIMPS could be further improved in two additional areas. First, the connecting-ducts adjacent to the expansion and compression-spaces should be modeled. The uncalibrated GLIMPS predictions for the SPRE would have been improved if a connecting-duct model existed. The SPRE has an unusually large connecting-duct between the cooler and compression-space. The surface area and volume of this connecting-duct had to be lumped with the compression-space in the SPRE model. Secondly, the parasitic losses should be an integral part of the GLIMPS thermodynamic simulation. These losses influence the predicted engine pressure waves.

Current plans are to continue the validation of GLIMPS and HFAST for the RE-1000 with various working fluids. Predictions will be generated for a kinematic Stirling engine and compared with experimental data. Results of this work will be described in a future NASA technical memorandum.

REFERENCES

1. J.G. Schreiber, S.M. Geng, and G.V. Lorenz, "RE-1000 Free-Piston Stirling Engine Sensitivity Test Results," NASA TM-88846, 1986.
2. J.E. Cairelli, "SPRE I Free-Piston Stirling Engine Testing at NASA Lewis Research Center," NASA TM-100241, 1987.
3. J. Corey, "Standards and Nomenclature for Reporting of Stirling Engine Performance," 24th IECEC, 1989, Vol. 5, pp. 2325-2329.
4. D. Gedeon, "A Globally-Implicit Stirling Cycle Simulation," 21st IECEC, 1986, Vol. 1, pp. 550-554.
5. D. Gedeon, "GLIMPS version 4.0 User's Manual," Gedeon Associates, 16922 South Canaan Road, Athens, OH 45701, 1992, (in press).
6. S.C. Huang, "HFAST: A Harmonic Analysis Program for Stirling Cycles," (To be published in: 27th IECEC, (number 92IECEC425), 1992).
7. K.P. Lee, "A Simplistic Model of Cyclic Heat Transfer Phenomena in Closed Spaces," 18th IECEC, 1983, Vol. 2, pp. 720-723.

REPORT DOCUMENTATION PAGE

Form Approved
OMB No. 0704-0188

1. AGENCY USE ONLY (*Leave blank*)	2. REPORT DATE	3. REPORT TYPE AND DATES COVERED
	1992	Technical Memorandum

4. TITLE AND SUBTITLE
Comparison of GLIMPS and HFAST Stirling Engine Code Predictions With Experimental Data

5. FUNDING NUMBERS
WU–590–13–11

6. AUTHOR(S)
Steven M. Geng and Roy C. Tew

7. PERFORMING ORGANIZATION NAME(S) AND ADDRESS(ES)
National Aeronautics and Space Administration
Lewis Research Center
Cleveland, Ohio 44135–3191

8. PERFORMING ORGANIZATION REPORT NUMBER
E–7078

9. SPONSORING/MONITORING AGENCY NAMES(S) AND ADDRESS(ES)
National Aeronautics and Space Administration
Washington, D.C. 20546–0001

10. SPONSORING/MONITORING AGENCY REPORT NUMBER
NASA TM–105549

11. SUPPLEMENTARY NOTES
Prepared for the 27th Intersociety Energy Conversion Engineering Conference cosponsored by SAE, ACS, AIAA, ASME, IEEE, AIChE, and ANS, San Diego, California, August 3–7, 1992. Responsible person, Steven M. Geng, (216) 433–6145.

12a. DISTRIBUTION/AVAILABILITY STATEMENT
Unclassified - Unlimited
Subject Category 85

12b. DISTRIBUTION CODE

13. ABSTRACT (*Maximum 200 words*)

Predictions from GLIMPS and HFAST design codes are compared with experimental data for the RE-1000 and SPRE free-piston Stirling engines. Engine performance and available power loss predictions are compared. Differences exist between GLIMPS and HFAST loss predictions. Both codes require engine-specific calibration to bring predictions and experimental data into agreement.

14. SUBJECT TERMS
Stirling engine; Heat engine; Stirling cycle; Free-piston stirling; Computer model; GLIMPS; HFAST

15. NUMBER OF PAGES
8

16. PRICE CODE
A02

17. SECURITY CLASSIFICATION OF REPORT	18. SECURITY CLASSIFICATION OF THIS PAGE	19. SECURITY CLASSIFICATION OF ABSTRACT	20. LIMITATION OF ABSTRACT
Unclassified	Unclassified	Unclassified	